

# White Rabbit-Based Time Distribution at NIST

J. Savory, J. Sherman, and S. Romisch  
Time and Frequency Division  
National Institute of Standards and Technology  
Boulder, CO 80305  
joshua.savory@nist.gov

**Abstract**— The National Institute of Standards and Technology (NIST) produces a real-time realization of UTC(NIST) which is used to contribute to Coordinated Universal Time (UTC) and as a source for accurate time in the USA. The atomic clocks contributing to the time scale ensemble, the time transfer systems used to contribute to UTC and the distribution system used to disseminate UTC(NIST) to remote users are located in different parts of the NIST campus, far from each other and from the UTC(NIST) reference point. Since the physical inputs to these systems are not collocated within the campus, an accurate and stable infrastructure for time signal distribution is required. Currently, the local delays need to be known with an uncertainty of a few hundreds of picoseconds to avoid compromising the ultimate accuracy of the time transfer link’s calibrations. Previously, coaxial cables or a commercial fiber-based frequency transfer system implemented by amplitude-modulation of a laser source were used to distribute signals between on-site locations, and clock trip calibrations were performed to measure the delays experienced by these signals [1]. The capability of WR-based time transfer systems to provide an on-time, accurate remote copy of its input pulse-per-second (PPS) signal made it a very appealing alternative to our previously implemented distribution system, which required time consuming re-calibration following instances of temporary signal interruptions. In this paper, we evaluate the use of WR-based time and frequency transfer within the NIST campus and verify its calibration procedure using a clock trip protocol [1].

**Keywords**—Time Transfer, White Rabbit

## I. INTRODUCTION

White Rabbit (WR) technology was initially developed at CERN, the European Organization for Nuclear Research, to produce a delay-compensated timing signal at remote locations for accelerator control and timing [2]. Information about the WR technology used at CERN is open source [3] and the hardware has been developed commercially. The base specifications of a calibrated WR time link are sub-nanosecond accuracy with picosecond stability, compatibility with commercial network hardware at fiber lengths of up to 10 km, and support for up to 1,000 nodes. The active compensation for the length and perturbations in the fiber is done using two-way time transfer through a combination of Precision Time Protocol (PTP) synchronization, Synchronous Ethernet (SyncE) synchronization and digital dual-mixer time difference phase detection.

At NIST, the time transfer systems used to contribute to UTC and the distribution system used to disseminate UTC(NIST) to remote users are located in different parts of the NIST campus,

far from each other and from the UTC(NIST) reference point. Pulse distribution over long distances through coaxial cable is prohibitive due to attenuation, environmental, and impedance issues [4]. In comparison with other time transfer technologies, WR links offer the additional advantage that they can be calibrated to remove the propagation delays and produce an on-time remote secondary reference plane that is synchronized with the primary reference plane. While less stable than high-performance fiber-based frequency transfer systems over short averaging intervals, WR links maintain phase continuity over disruptions in the primary reference signal, and exhibit better long-term time stability. To determine the feasibility of using WR-based time transfer at NIST, its frequency and time stability were evaluated using a loopback measurement between two buildings on campus; environmental sensitivity of the master and remote transceivers were evaluated using an environmental chamber; and the calibration accuracy was evaluated by comparing it to several clock trip calibrations.

## II. NIST’S WHITE RABBIT FIBER LINK LAYOUT

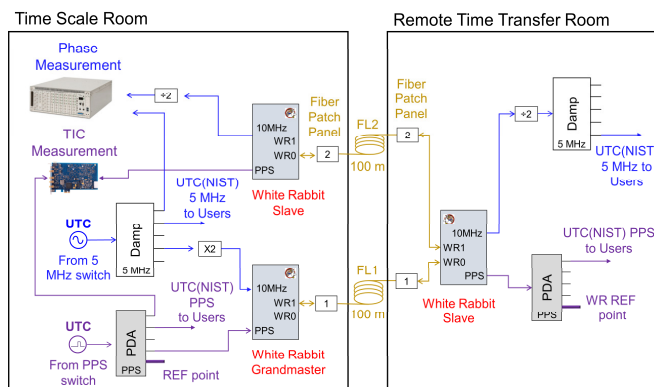


Fig. 1. Layout of the WR transfer system used to distribute time and frequency from the NIST timescale room to the remote time transfer room. The following items are abbreviated in the figure: Pulse Distribution Amplifier (PDA), Distribution Amplifier (Damp), and Coordinated Universal Time (UTC).

The WR link deployed at NIST uses the WR-LEN modules produced by Seven Solutions\*. For the purposes of this work, a WR time link consists of a grandmaster module, which is sourced with a local 10 MHz and a pulse-per-second (PPS) reference, a slave module which outputs a 10 MHz and a PPS signal at a remote location and a single (bi-directional) fiber connecting the two modules. Each time module contains two laser ports: a module can be configured to act as a slave on one port and master on another allowing modules to be daisy

chained. The network hardware implemented in the NIST link has the grandmaster and master modules transmitting at a wavelength of 1310 nm, and the slave modules transmit at 1550 nm.

The layout of the WR fiber link at NIST is shown in Fig. 1. The link runs approximately 100 meters between the NIST time scale room and time transfer room where the time transfer equipment is housed. A WR grandmaster module, located in the time scale room, is sourced with a 10 MHz and a PPS signal directly from the UTC(NIST) signal plane. The grandmaster module is connected by Fiber Link 1 (FL1) to a remote slave module in the time transfer room, which reproduces the UTC(NIST) PPS and 10 MHz signals. These signals are used to source a TWSTFT (Two-Way Satellite Time and Frequency Transfer) Earth station and GPS (Global Positioning System) receiver for dissemination of UTC(NIST). The second fiber port on the remote WR module is run in master mode and is used to connect back to a local slave module in the time scale room via Fiber Link 2 (FL2). The outputs of this module are used for monitoring and for performing stability measurements of the WR link.

### III. TIME TRANSFER SYSTEM COMPARISON

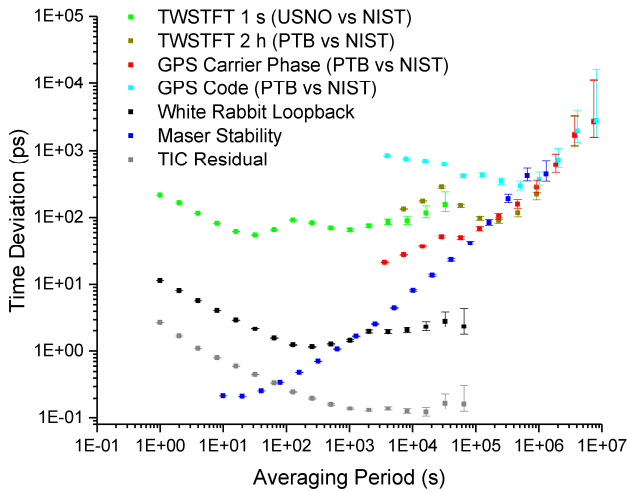


Fig. 2. Comparison of the time deviation (TDEV) as function of averaging period between several time transfer systems at NIST. The WR loopback PPS measurement (see Fig. 1) is shown in black and the residual of the time interval counter used to perform this measurement is shown in gray. Also shown are a TWSTFT comparison of UTC(NIST) and UTC(USNO) at a time interval of 1 s (green), a TWSTFT comparison of UTC(NIST) vs UTC(PTB) at a time interval of 2 h (dark green), a comparison of UTC(NIST) vs UTC(PTB) via GPS code (cyan) and carrier phase (red), and a typical maser stability (blue).

The stability of the transmitted PPS was evaluated over the course of several days by comparing the UTC(NIST) PPS and the returning WR link's PPS on a GuideTech (GT668PCIe-1)\* time interval counter as shown in Fig. 1. A comparison of this measurement to typical results from NIST's GPS and TWSTFT links can be seen in Fig. 2. The stability of the GPS and TWSTFT links are measured through time scale comparisons, and therefore also contain the noise of the scales themselves. The transfer system noise will dominate in the short-term and the scale-to-scale noise determines the long-term performance of the comparison. A typical maser stability

is also included in this plot to show approximately at what averaging period the clock noise dominates, thus allowing the clock signal to be transferred without corruption. The WR link PPS's stability is below 20 ps at all averaging periods, and is below the clock noise for averaging periods greater than 1000 s. Furthermore, as the short-term noise of the WR link is white phase it is well below the minimum time deviation (TDEV) of GPS carrier phase ( $\sim 20$  ps) for averaging periods greater than 10 s.

### IV. LONG-TERM FREQUENCY STABILITY EVALUATION

The WR link's stability is continually monitored by dividing the 10 MHz signal from the local WR slave module to 5 MHz and comparing it with the UTC(NIST) 5 MHz signal (see Fig. 1) on a multichannel dual-mixer phase measurement system from Microchip (TSC 12030)\*. A measurement of the phase difference for the loopback over  $\sim 100$  days is shown in Fig. 3 and a phase drift of approximately 40 ps is observed. This corresponds to a long-term frequency offset of  $\sim 5 \times 10^{-18}$  and sets the frequency accuracy of the link. The observed phase drift appears to be decreasing in magnitude in the last 20 days of data and could be due to aging in any one of the components (isolation amplifiers, frequency divider, frequency doubler, WR hardware, etc.) involved in the measurement chain. With this performance, in order to ensure that the secondary reference point's time offset is within 200 ps of UTC(NIST), the WR link should be recalibrated at least once a year.

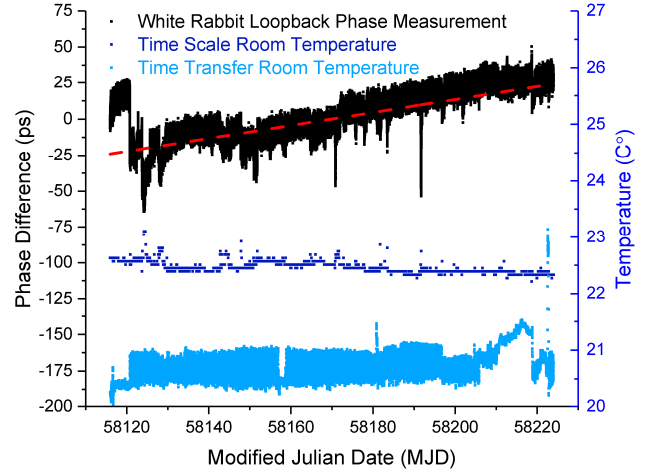


Fig. 3. Plot of the long-term phase difference (left axis) over time of the White Rabbit 10 MHz loopback is shown in black and the temperatures (right axis) of the time scale and time transfer rooms are shown in dark blue and light blue respectively.

The modified Allan deviation (MDEV) of the loopback phase data is shown in Fig. 4 together with that of a typical maser signal at a measurement bandwidth of 0.1 Hz (10 s). After 500 s of averaging, a maser signal would be observable on the 10 MHz WR link as the link noise at this averaging interval is below the noise of the maser. The link stability is  $\sim 1 \times 10^{-16}$  after 100,000 s of averaging and has not yet reached the flicker floor. However, the overall frequency accuracy of the link will be set at  $\sim 5 \times 10^{-18}$  by the phase drift observed in Fig. 3.

In Fig. 3, a correlation is observed between phase excursions in the loopback measurement and fluctuations in temperature of

the room which houses the WR modules. The WR module's case is designed to be the heat sink for the module itself, hence the observed temperature dependence. In the next section, the environmental sensitivity of the time modules is explored in a more controlled setting.

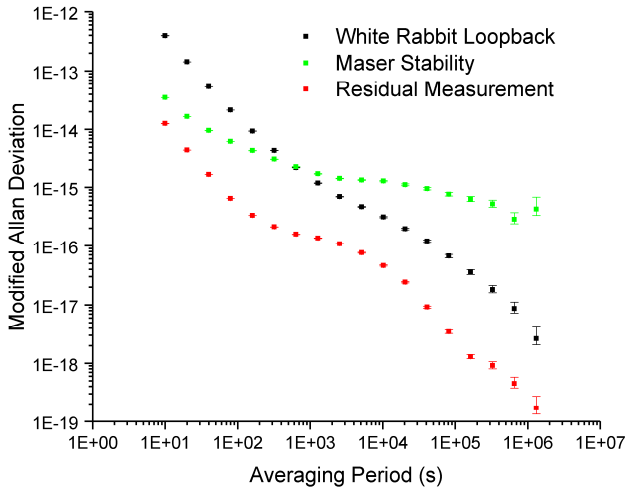


Fig. 4. Comparison of the modified Allan deviation (MDEV) as a function of averaging period for the WR link 10 MHz loopback (black) measurement, a typical maser stability (green) and a residual measurement (red) performed on the phase measurement system used to collect both sets of phase data.

## V. ENVIRONMENTAL SENSITIVITY MEASUREMENTS

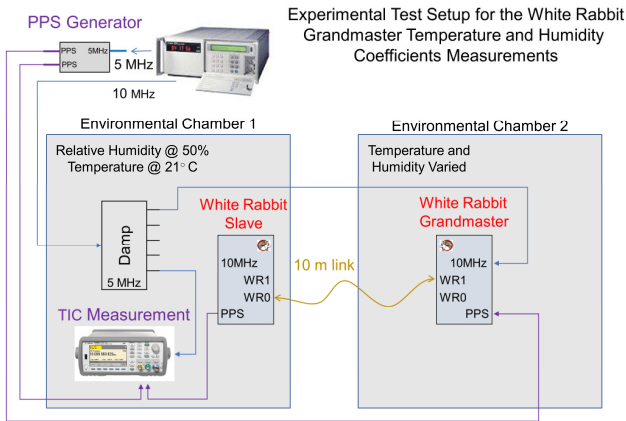


Fig. 5. Test setup used to evaluate the WR grandmaster modules' environmental sensitivity.

To quantify the WR time modules' environmental sensitivities, two modules were placed in separate environmental chambers. The experimental setup used to evaluate the grandmaster module is shown in Fig. 5. The grandmaster module was sourced with synchronous PPS and 10 MHz signals from a 5071A Cesium clock from Microchip\* and placed in the test environmental chamber whose temperature and humidity were varied. The slave module was connected to the grandmaster module using a 10 m fiber link and placed in the control chamber which remained static in temperature and humidity for the duration of the test. The phase change in the WR slave module PPS against the source PPS was measured on a time interval counter from Spectracom (Pendulum CNT-91)\*. To determine the temperature coefficient, the test chamber was

varied by 2°C steps (21°C to 23°C and back). Similarly, to measure the humidity coefficient the humidity in the test chamber was stepped in increments of 10% RH (50% RH to 60% RH and back). In both cases, the chamber was left at each temperature and humidity setting for a time interval of at least 1 day. A similar test setup was used to evaluate the environmental sensitivity of the WR slave module in which the slave module was placed in the test chamber and the grandmaster in the control chamber.

The results of these measurements are summarized in Table 1. No significant humidity coefficient was observed for either the grandmaster or slave module. However, a large temperature coefficient of 29 ps/°C was observed for the grandmaster module, which is approximately seven times larger than the one for the slave module and that of a typical isolation amplifier (5 ps/°C). This result coincides with the temperature correlation observed in Fig 3, which shows a sensitivity bias towards the time scale room's temperature.

MODULE ENVIRONMENTAL SENSITIVITY

Module	Temperature Coefficient	Humidity Coefficient
Grandmaster	29.0(2) ps/°C	0.41(3) ps/%
Slave	4.0(2) ps/°C	0.04(2) ps/%

Table 1. Table of measured WR time module phase sensitivity to changes in temperature ( $P_t$ ) and humidity ( $P_h$ ).

## VI. TIME OFFSET CALIBRATION

The WR link must not only be stable but accurate as well. The WR modules allow for the alignment in time of the PPS at the primary and secondary reference points. To accomplish this the WR time modules were initially calibrated according to the procedure in [5] to remove time offsets in the WR link due to fiber length and internal electrical delays. To account for external delays in the PPS distribution chain and align the primary and secondary reference points, clock trip [6, 7, 8] and WR trip measurements were performed to determine the remaining PPS delays. The value from these measurements were programmed into WR grandmaster and slave module to do the final alignment.

In a clock trip, a traveling clock is moved between the primary and secondary reference point, and the time difference between the reference point and the traveling clock is measured at each location. Using prior information about the traveling clock's frequency and stability, the time offset between the two reference points and the associated uncertainty can be calculated. By comparing the time difference between the traveling clock and the primary reference point measured at the beginning and end of each clock trip, the measurement's systematics can be accessed in what is called the closure measurement. A successful closure measurement should be statistically consistent with zero. The full details of this procedure and measurement parameters used in this work are in [1].

Similarly, a WR calibration trip consists of using a grandmaster and slave pair of WR time modules to measure a secondary point against a primary reference point. In this procedure, the grandmaster WR time module is sourced by a PPS and a 10

MHz synchronous with the primary reference signals at the primary reference point's location where it remains for the duration of the measurement. Initially, the slave module is connected to the grandmaster using a local fiber (fiber A) and the initial time difference ( $\Delta\theta_I$ ) between the slave's PPS output and the primary reference point's PPS are measured on a time interval counter. The slave module is then moved to the location of the secondary reference point connected to the grandmaster using a second calibration fiber link (fiber B) and the mid-point time difference ( $\Delta\theta_M$ ) between the slave's PPS output and the secondary reference point's PPS is measured at the remote location. For the closure measurement, the slave module is then returned to the location of the primary reference point and the final time difference ( $\Delta\theta_F$ ) between the slave's PPS output and the primary reference point's PPS is measured. The time offset ( $D$ ) of the secondary reference point is calculated from these measurements

$$D = \Delta\theta_M - \frac{\Delta\theta_I + \Delta\theta_F}{2}. \quad (1)$$

The closure ( $C$ ) of the WR trip can be expressed as

$$C = \Delta\theta_F - \Delta\theta_I \quad (2)$$

and the uncertainty is simply the propagated error of the time difference measurements. The WR trip is simpler than the clock trip because no time prediction is required as the WR link time signals are synchronous with the primary reference signals.

The time difference measurements for the WR trip were all performed with a time interval counter from Spectracom (Pendulum CNT-91)\*. Each time interval measurement was averaged over a period of 100 s which corresponds to a statistical uncertainty of  $\sim 4$  ps at this average period (see Fig. 2). At each location, the link was re-established and the modules' temperature allowed to settle for at least 30 minutes before performing the time difference measurements. After the initial calibration, the WR link's time delay is to first order independent of the fiber link length. To further reduce this error the lengths of the two calibrations fibers (A and B) were chosen to be approximately equal.

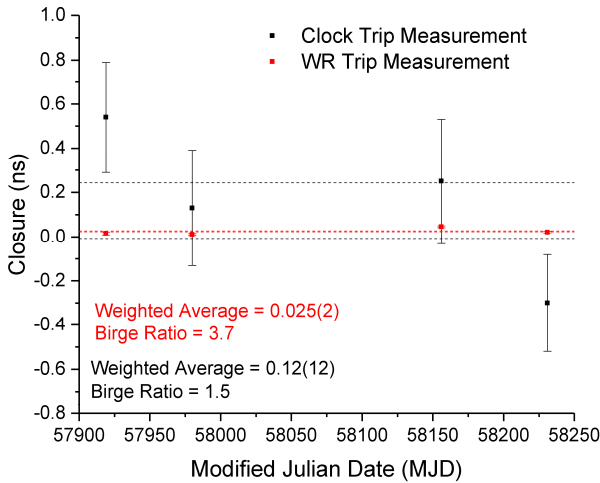


Fig. 6. Result of the closure measurements at the MJD they were performed for clock trip (black) and WR trip (red) protocols.

The following WR trip and clock trip measurements were performed to validate a successful recalibration of the WR link and to evaluate the calibration methods. The measurements were performed at different dates and should be viewed as independent and not as a reflection of the link's stability. A comparison of the closure measurements obtained for the clock trip and WR trip calibrations are shown in Fig. 6. As previously observed in [1], the clock trip's closure measurements are statistically consistent with zero and have a Birge ratio consistent with  $\sim 1$  based on a small number of measurements [9]. On the other hand, the WR trip measurements have a significant non-statistical bias and non-statistical scatter (Birge ratio  $\gg 1$ ). To account for this the WR time offset uncertainties are scaled by the Birge ratio (3.7) and summed with half of the associated closure measurement. The most likely contributor to the observed bias and scatter is the large temperature coefficient of the grandmaster module. During the calibration process, it is difficult to maintain a constant case temperature as the equipment is moved between different locations and the link re-established.

For both methods, the time offset measurements of the secondary reference point in the time transfer room are shown in Fig. 7. At all measurement dates and with both methods the measured time offset was less than 200 ps and in most cases statistically consistent with the zero. Despite being scaled based on the closure measurements, the uncertainties for the WR trips are still a factor of  $\sim 5$  smaller than the clock trip uncertainties. The difference between the time offsets measured with the two protocols is shown in Fig. 8. No statistically significant bias between the two methods is observed at the one sigma level. Based on a conservative interpretation of these results, the WR trip protocol can be used to calibrate the WR link at sub-100 ps accuracies with a single measurement. If the systematics of a WR trip can be better constrained, time offset measurements at the 10 ps level should be possible.

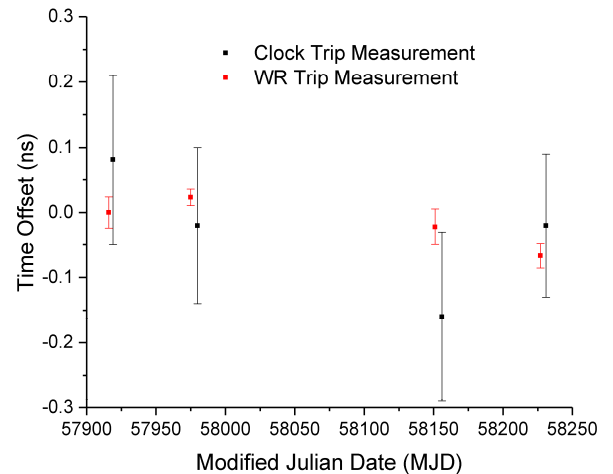


Fig. 7. Result of the time offset measurements of the time transfer room reference point at the MJD they were performed for clock trip (black) and WR trip (red) protocols.

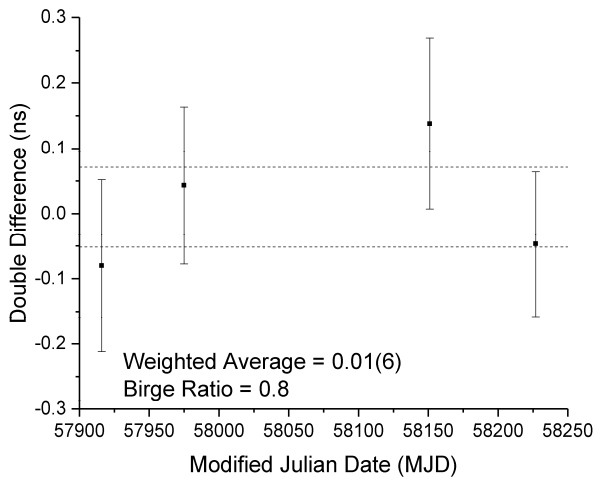


Fig. 8. Time offset difference obtained with the two different calibration protocols (WR trip – clock trip) at the MJD they were performed for the time transfer room reference point.

## VII. CONCLUSIONS

The WR hardware has met the accuracy and stability requirements to provide UTC(NIST) to the time transfer systems used to contribute to UTC that are in different locations on the NIST campus. Measurements performed on the PPS WR loopback show that WR link's time stability is below 20 ps at all averaging periods, and thus stable enough to distribute UTC(NIST) throughout the NIST campus. Time offset measurements done with the clock and WR trips calibration protocol are in high agreement and demonstrate that WR link can be calibrated and measured to an accuracy of < 100 ps. Furthermore, a long-term measurement of the 10 MHz WR loopback shows a frequency accuracy of  $\sim 5 \times 10^{-18}$  which means that WR link need only be recalibrated once a year. The WR trip protocol has also been investigated and shown to offer an alternative method to calibrate remote reference points with a factor of five smaller uncertainties than that of a clock trip. The accuracy and stability of the WR modules could be further improved by reducing the temperature coefficient of the grandmaster module which is currently under evaluation [10].

## DISCLAIMER

This paper includes contributions for the U.S. Government and it is not subject to copyright.

\* Certain commercial equipment, instruments, or materials are identified in this paper for informational purposes only. Such identification does not imply recommendation or endorsement by the National Institute of Standards and Technology, nor does it imply that the materials or equipment identified are necessarily the best available for the purpose.

## ACKNOWLEDGMENTS

The authors would like to thank Tom Parker, Bijunath Patla, Jian Yao, and Victor Zhang for providing data on the NIST time transfer systems.

## REFERENCES

- [1] J. Savory, S. Romisch, L. Hernandez, and K. Maurer, "Local Distribution and Calibration of Timing Signals at NIST," Proceedings of the 48th Annual Precise Time and Time Interval Systems and Applications Meeting, Monterey, California, pp. 326–342, January 2017.
- [2] J. Serrano, P. Alvarez, M. Cattin, E. Garcia Cota, J. Lewis, P. Moreira, T. Wlostowski, G. Gaderer, P. Loschmidt, J. Dedič, R. Bär, T. Fleck, M. Kreider, C. Prados, and S. Rauch, "THE WHITE RABBIT PROJECT", Proceedings of the 12th International Conference On Accelerator And Large Experimental Physics Control Systems, Kobe, Japan, pp. 93–95, October 2009.
- [3] White Rabbit Open Hardware Repository: Technical Presentations <https://www.ohwr.org/projects/white-rabbit>.
- [4] M. Siccardi, D. Rovera, and S. Romisch, "Delay measurements of PPS signals in timing systems", *Frequency Control Symposium (IFCS)*, 2016 IEEE International, New Orleans, LA, 628, May 2016.
- [5] G. Daniluk. (2014, Aug. 13). White Rabbit Calibration Procedure Version 1.0, CERN BE-CO-HT [Online]. Available: <http://www.ohwr.org/documents/213>.
- [6] L. N. Bodily and R. C. Hyatt, "'Flying Clock' Comparisons Extended to East Europe, Africa and Australia", *Hewlett-Packard Journal*, 19, 12, 1967.
- [7] H. Hellwig and A. E. Wainwright, "A portable rubidium clock for precision time transport," *Proceedings of the 7th Annual Precise Time and Time Interval Systems and Applications Meeting*, Washington, D.C., 143, December 1975.
- [8] L. G. Rueger and R. A. Nelson, "Portable Hydrogen maser clock time transfer at the subnanosecond level," *Proceedings of the 19th Annual Precise Time and Time Interval Systems and Applications Meeting*, December 1987.
- [9] T. Parker "Update on a Comparison of Cesium Fountain Primary Frequency Standards" *2011 Joint Conference of the IEEE International Frequency Control Symposium and European Frequency and Time Forum*, San Francisco, July 2011.
- [10] White Rabbit Open Hardware Repository: WRS Low Jitter Daugherboard <https://www.ohwr.org/projects/wrs-low-jitter/wiki>.